



Capturing yield surface evolution with a multilinear anisotropic kinematic hardening model



Meijuan Zhang, Jose María Benítez, Francisco Javier Montáns*

Escuela Técnica Superior de Ingeniería Aeronáutica y del Espacio, Universidad Politécnica de Madrid, Plaza Cardenal Cisneros 3, 28040 Madrid, Spain

ARTICLE INFO

Article history:

Received 3 July 2015

Revised 19 October 2015

Available online 11 December 2015

Keywords:

Plasticity

Yield surface evolution

Anisotropic hardening

Multisurface plasticity

ABSTRACT

Many authors have observed experimentally that the macroscopic yield surface changes substantially its shape during plastic flow, specially in metals which suffer significant work hardening. The evolution is frequently characterized by a corner effect in the stress direction of loading, and a flatter shape in the opposite direction. In order to incorporate this effect many constitutive models for yield surface evolution have been proposed in the literature. In this work we perform some numerical predictions for experiments similar to the ones performed in the literature using a multilayer kinematic hardening model which employs the associative Prager's translation rule. Using this model we prescribe offsets of probing plastic strain, so apparent yield surfaces can be determined in a similar way as it is performed in the actual experiments. We show that similar shapes to those reported in experiments are obtained. From the simulations we can conclude that a relevant part of the apparent yield surface evolution may be related to the anisotropic kinematic hardening field.

© 2015 Elsevier Ltd. All rights reserved.

1. Introduction

Classical phenomenological theories of plasticity for metals are based on the existence of an elastic domain characterized by a yield surface. For polycrystal isotropic metals, the Maxwell–von Mises yield criterion has been verified by a number of authors, starting with the tension–torsion experiments of Taylor and Quinney (1932). This yield surface is a circle in the $(\sigma - \sqrt{3}\tau)$ tension stress σ –torsion stress τ plane and in the deviatoric stress “ π ” plane. However, for at least some hardening materials, upon plastic straining in one direction the measured yield surface not only translates due to kinematic hardening, but also changes its shape. This change of shape has been observed by many authors in different metals, see Theocaris and Hazell (1965), Kuwabara et al. (2000), Ishikawa (1997), Ishikawa and Sasaki (1989), Khan et al. (2009, 2010a, 2010b); Hu et al. (2015); 2014), Wu and Yeh (1991), Wu (2003), Sung et al. (2011), Kim et al. (2009), Rousset (1985), Rousset and Marquis (1985), Benallal and Marquis (1987), among others. As observed in these experiments, the actual shape of the measured yield surface depends on several factors as the material itself, the amount of prestress, and the permanent plastic strain (probing strain) after which the onset of plasticity (i.e. the limit of the elastic domain) is established. The relevance of

this change of shape is unquestionable because it largely affects non-proportional loading and the springback behavior.

Many experiments show similar conclusions on the evolution of the measured shape of the yield surface. Upon prestressing in one direction in the $\sigma - \sqrt{3}\tau$ (axial–torsion) plane, the yield surface shows a “nose” in that direction and an almost flat line in the opposite direction (Khan et al., 2009, 2010a, 2010b; Hu et al., 2014, 2015, Wu and Yeh, 1991; Rousset, 1985; Rousset and Marquis, 1985; Benallal and Marquis, 1987), resulting in an often named “egg” effect (Lemaitre and Desmorat, 2005). This nose (and the opposite flat part) changes according to new substantial prestressing. Some experiments have also observed that in the direction perpendicular to the prestressing one (in the axial–torsion plane) the measured elastic domain becomes wider than in the direction of pre-loading (Ishikawa, 1997; Ishikawa and Sasaki, 1989; Khan et al., 2009, 2010a, 2010b; Hu et al., 2014, 2015; Wu and Yeh, 1991; Rousset, 1985; Rousset and Marquis, 1985; Benallal and Marquis, 1987). Furthermore, although it is rarely accentuated (usually neglected) some experiments also show symmetric slightly concave parts in the surface behind the nose, an effect clearly seen in the experimental data of Wu and Yeh (1991) and also present in some of the tests of Khan et al. (2009, 2010a, 2010b).

Because of the major importance of all these effects, many material models have been proposed or extended in order to account for the shape evolution of the yield surface. Some of the models are phenomenological (Helling and Miller, 1987, 1988; Kurtyka and Życzkowski, 1996; Voyiadjis and Foroozesh, 1990; François, 2001; Liu et al., 2011; Wu and Hong, 2011; Lee et al., 2012; Radi and Abdul-Latif, 2012; Barlat et al., 2013; Shi et al. (2014)) and some of

* Corresponding author. Tel.: +34 637 908 304.

E-mail addresses: meijuan.zhang@alumnos.upm.es (M. Zhang), josemaria.benitez@upm.es (J.M. Benítez), fco.montans@upm.es (F.J. Montáns).

them micromechanically-based or motivated (Zattarin et al., 2004; Kabirian and Khan, 2015; Yoshida et al., 2014; Hu et al., 2015). These models are substantially more complex than traditional models (Lemaitre and Desmorat, 2005) and despite of their complexity, they are usually not able to capture some details. Probably a recent crystal plasticity model is the first one to capture small concavities sometimes present in experiments (Hu et al., 2015).

The purpose of this paper is to perform some predictions of experiments to detect *apparent* yield surfaces employing a special multilinear (or multilayer) nested yield surfaces model. The model is based on the original ideas of Iwan (1967) and Mroz (1969), Montáns (2000) of employing several nested yield surfaces that discretize the uniaxial stress–strain curve. The procedure does not require any parameter-fitting procedure; the prescribed stress–strain data are exactly captured in the uniaxial case in a similar way as in our hyperelastic (Latorre and Montáns, 2013; Latorre and Montáns, 2014b) and damage models (Miñano and Montáns, 2015). From a theoretical standpoint, there is a clear and remarkable difference of our model with the Mroz proposal. In our case the outer surfaces are *not* yield surfaces, but only hardening surfaces; i.e. they are simply a tool to compute the effective anisotropic hardening modulus. The actual yield surface is always the innermost one. The plastic strains are always normal to that yield surface and the hardening direction of the yield surface follows Prager's associative hardening rule. From a computational standpoint, whereas for the Mroz model there are some relevant restrictions when formulating a fully implicit closest point projection algorithm (Montáns, 2000; Caminero and Montáns, 2006; Montáns and Caminero, 2007), in the case of Prager's rule a closest point projection algorithm is possible without restriction, and this algorithm reduces to the solution of a nonlinear scalar function (Montáns, 2001; Montáns, 2004). Furthermore, it is remarkable that in the case of linear kinematic hardening, the model exactly reduces to classical J_2 -plasticity regardless of the number of surfaces employed (Montáns and Caminero, 2007) not only from a theoretical but also from a computational point of view (i.e. the global iterations are the same up to round-off errors).

Therefore, during the predictions given below, we note that the actual (analytical) yield surface is always the same, i.e. the innermost von Mises surface. Both the plastic flow and the hardening (i.e. translation of the yield surface) follows associative rules. The stress-driven simulations have been performed using a fully implicit algorithm with very small steps and a restrictive tolerance. However, we show that employing the typical probing plastic strains and directions we observe *apparent* (measured) yield surfaces with similar characteristics as those observed in experiments; i.e. a “nose” in the preloading direction, a more flat surface in the opposite direction, a relatively wider “elastic” domain in a direction perpendicular to the preloading direction and even small concave zones behind the nose.

It is obvious that yield surface evolution may be due to many different aspects as isotropic hardening, texture evolution (Caminero et al., 2011; Montáns et al., 2012), ratcheting (Lemaitre and Chaboche, 1994), etc. Viscous effects and yield stress relaxation may also have an important impact on the observed yield surfaces. However, we will not include these effects, but only anisotropic kinematic hardening. The purpose of this work is to show that a relevant part of the observations in the experiments may be attributed to (and hence modeled by) anisotropic kinematic hardening developed during preloading.

2. Summary of the model

The main objective of the model is to account for multiaxial nonlinear anisotropic kinematic hardening during nonproportional loading. In order to meet this goal, several nested (initially concentric) surfaces are employed. The innermost one is the yield surface, the boundary of the elastic domain, taken as the von Mises one

$$f_1 := \|\sigma^d - \alpha_1\| - r_1 \leq 0 \quad (1)$$

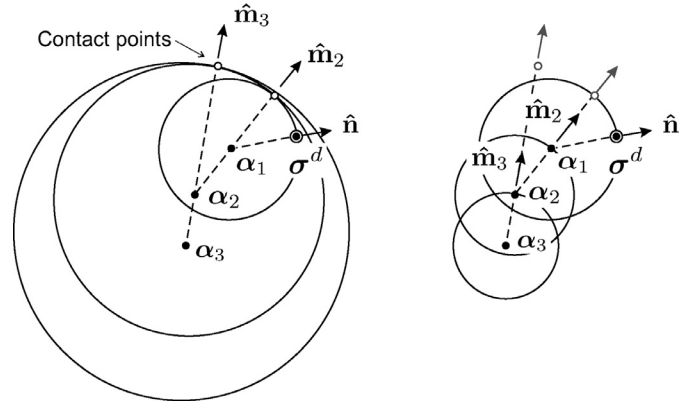


Fig. 1. Geometric relations of the model in the deviatoric plane. Left: stress tensor σ^d , flow direction \hat{n} , hardening surfaces f_i , contact points and translation directions \hat{m}_i . Right: equivalent surfaces f_i .

where σ^d is the deviatoric stress tensor, α_1 is the backstress tensor, $\|\cdot\|$ is the Euclidean norm and $r_1 = \sqrt{2/3}\sigma_Y$ is the radius of the yield surface for the corresponding yield stress σ_Y (Fig. 1). We apply the principle of maximum dissipation and assume associativity of both the plastic flow and of the hardening, i.e.

$$\dot{\epsilon}^p = \dot{\gamma} \frac{\partial f_1}{\partial \sigma} = \dot{\gamma} \hat{n} \quad \text{and} \quad \dot{\alpha}_1 = -\dot{\lambda} \frac{\partial f_1}{\partial \alpha_1} = \dot{\lambda} \hat{n} \quad \text{with} \quad \hat{n} := \frac{\sigma^d - \alpha_1}{\|\sigma^d - \alpha_1\|} \quad (2)$$

where $\dot{\epsilon}^p$ is the plastic strain rate and $\dot{\alpha}_1$ is the rate of the backstress, which translates according to the associative Prager's rule. The multipliers $\dot{\gamma}$ and

$$\dot{\lambda} \equiv \langle \dot{\alpha}_1 : \hat{n} \rangle = \|\dot{\alpha}_1\| \quad (3)$$

are computed from the hardening pattern and the consistency condition. Let \bar{H} be the effective hardening modulus. Then we have the usual relation

$$\dot{\lambda} = \frac{2}{3} \bar{H} \dot{\gamma} \quad \text{so} \quad \dot{\gamma} = \frac{\dot{\lambda}}{\frac{2}{3} \bar{H}} = \frac{\|\dot{\alpha}_1\|}{\frac{2}{3} \bar{H}} \quad (4)$$

and Prager's rule results in

$$\dot{\alpha}_1 = \frac{2}{3} \bar{H} \dot{\gamma} \hat{n} \quad (5)$$

From the constitutive equation for the deviatoric stress rate, using Eq. (2)

$$\dot{\sigma}^d = 2\mu (\dot{\epsilon}^d - \dot{\epsilon}^p) = 2\mu \dot{\epsilon}^d - 2\mu \dot{\gamma} \hat{n} \quad (6)$$

where $\dot{\epsilon}^d$ are the deviatoric strain rates and μ is the shear modulus. The consistency conditions are

$$\begin{cases} f_1 = 0, \dot{f}_1 = 0 & \text{if } \dot{\gamma} > 0 \\ f_1 \leq 0 & \text{if } \dot{\gamma} = 0 \end{cases} \quad (7)$$

Using $\partial f_1 / \partial \sigma = -\partial f_1 / \partial \alpha_1 = \hat{n}$, we readily obtain the consistency parameter

$$\dot{f}_1 = 0 \Rightarrow \hat{n} : (\dot{\sigma}^d - \dot{\alpha}_1) = 0 \Rightarrow \dot{\gamma} = \frac{2\mu \langle \hat{n} : \dot{\epsilon} \rangle}{2\mu + \frac{2}{3} \bar{H}} \quad (8)$$

The elastoplastic tangent moduli \mathcal{C}^{ep} relate stress rates $\dot{\sigma}$ with total strain rates $\dot{\epsilon}$ by $\dot{\sigma} = \mathcal{C}^{ep} : \dot{\epsilon}$. These moduli are obtained from the same classical expression employing Eq. (8) in the constitutive equation of the deviatoric stress rates $\dot{\sigma}^d$

$$\dot{\sigma}^d = 2\mu \dot{\epsilon}^d - 2\mu \dot{\gamma} \hat{n} = 2\mu \dot{\epsilon}^d - \frac{2\mu^2 \langle \hat{n} : \dot{\epsilon} \rangle}{2\mu + \frac{2}{3} \bar{H}} \hat{n} \quad (9)$$

Download English Version:

<https://daneshyari.com/en/article/277221>

Download Persian Version:

<https://daneshyari.com/article/277221>

[Daneshyari.com](https://daneshyari.com)